NEW NEUTRON DIFFRACTION DATA CAPABILITY IN THE PDF-4+ 2014 RELATIONAL DATABASE

J. Faber, Faber Consulting, Thornton, PA 19373 USA

C. Crowder, J. Blanton, S. Kabekkodu, O. Gourdon*, T. Blanton and T. Fawcett, International Centre for Diffraction Data (ICDD), Newtown Square, PA 19073 USA

* present address: Los Alamos National Laboratory, Los Alamos, NM, 87545, USA

ABSTRACT

Neutron powder diffraction is a useful tool because elemental scattering contrast is quite different when compared to X-rays. Elements in the periodic table often have quite different scattering amplitudes. Unlike standard laboratory x-ray sources, neutrons are available both at nuclear reactors and pulsed sources. These facilities are available world-wide. In this paper, we treat the constant wavelength (CW) neutron case and calculate neutron powder diffraction patterns for ~241,000 entries with atomic coordinates in the PDF-4+ 2014. The calculation of I/I_c for quantitative phase analysis has also been carried out. Normalized total pattern index, Hanawalt, Fink and Long8 searches are available for search/match.

INTRODUCTION

The fundamental underpinnings for qualitative and quantitative phase analysis have rested with the description of diffraction results in terms of a concise peak-list, that is, d-spacing/peak intensity pairs. However, these reduced data (d,I pairs) do not conserve the full pattern information content (amorphous scattering, stress/strain and particle size effects). Recently, we have used on-the-fly technology to calculate fully digitized diffraction patterns for all entries in the PDF-4 (Faber, Fawcett (2002); Faber (2004)). The (d,I pairs) are commonly associated with PDF-2 data. On-the-fly technology allows us to calculate fully digitized patterns that are associated with PDF-4 data. A selection of peak shape profile functions allow us to match instrument calibration and experimental data (including the effects of crystallite size and strain). In this paper we report the population of PDF-2 and PDF-4 data for constant wavelength (CW) neutron scattering sources.

To continue this initiative, we have taken into account neutron diffraction data from constant wavelength (CW) sources. To accurately express the scattering in neutron diffraction experiments, we consider the wavelength of the incident beam flux-on-sample, the energy dependence of the sample absorption cross section, the precise details of the cylindrical sample geometry (Debye-Scherrer with sample diameter and packing fraction), and the instrumental resolution function.

We should note that the method does not account for amorphous phases. However, as experimental neutron data are submitted to the ICDD, amorphous phases will also be added to the database. Moreover, to the extent that small crystallite size formalisms can be used to approximate amorphous scattering, DDView+ (PDF-4 front end) allows us to model this behavior.

Unlike the laboratory X-ray case, where the incident beam wavelength is restricted to characteristic radiation values, the selected neutron source energy is taken relative to a Maxwellian component in the source spectrum (although for pulsed neutron sources the range of useful energies often extends into the epi-thermal region of the spectrum). One parameter is the relative scattering power of the unknown sample when compared to the intensity of a reference standard (usually corundum, Al_2O_3). It is useful to explore I/I_c for both X-ray and neutron scattering experiments. This is also relevant for X-ray experiments that utilize synchrotron radiation sources since a photon energy is selected from the white beam.

MATHEMATICAL BASIS FOR FLUX ON SAMPLE

For simulated powder patterns we take the X-ray expressions from (Hubbard, et. al. (1976)). Using the internal standard method, corundum, Al_2O_3 is selected as the reference material for the I/I_c method. I/I_c is defined as a ratio of the strongest line of corundum for a 1:1 mixture by weight of the two phases. More recently, POWD12 (Clark, et. al., (1973)) used the integrated intensity measure of all the peaks in the unknown compared to corundum. This is called the Reference Intensity Ratio. In addition to the 500 or so reference powder patterns from which the method has been built, the ICDD PDF-4+ now contains over 241,000 patterns with I/I_c calculated from structural data for X-rays and neutrons. For the X-ray case, the following can be applied for Bragg-Brentano flat plate geometry:

$$P_i = \left(\frac{P_o}{32\pi R}\right)\left(\frac{e^4}{m^2c^4}\right)\left(\frac{\lambda^3 M\left[F_T\right]^2}{2\mu V^2}\right)\left(\frac{1+\cos^2 2\theta}{\sin^2\theta\cos\theta}\right) \quad (1)$$

$$K = \left(\frac{P_0}{32\pi R)}\right)\left(\frac{e^4}{m^2c^{4)}}\right)\lambda^3$$

$$\frac{I^{abs}}{K} = \frac{MLp\left[F_T\right]^2}{2\mu V^2} = \gamma I^{rel}$$

$$\frac{I}{I_c} = \frac{\mu\gamma\rho_c}{\mu_c\gamma_c\rho}, \text{where subscript c is corundum}$$

In Eq.1, the first bracket contains the source dependent terms, the second is the Thompson one-electron scattering, the third is the sample dependent terms and the incident wavelength, and the last is the Lorentz-Polarization factor.

For the neutron case and cylindrical geometry, the power per unit length is given by (Bacon, 1975):

$$\frac{P}{I_o} = \left(\frac{\lambda^3 l_s}{8\pi r}\right)\left(\frac{V\rho'}{\rho}\right)\left(\frac{jN_c^2F^2}{\sin 2\theta\sin\theta}\right)e^{-2W}A_{hkl} \quad (2).$$

In Eq. 2, the first term contains incident geometry and incident wavelength, the second contains the actual sample volume corrected for packing density, the third contains the multiplicity, j, and the Lorentz factor. A_{hkl} is the absorption factor (energy dependent). The apparent density compared to the theoretical density, ρ'/ρ becomes the packing fraction for the powder in a cylindrical container. This equation requires normalization since we do not know the incident beam flux-on-sample or the detector efficiency. We choose λ=1.5406 Å as the reference state so that I/I_c =1.0 for corundum at that wavelength.

We see from Equations 1 and 2 that the scattering power of the sample increases as λ^3 . Absorption is also energy dependent.

CALCULATION OF THE LINEAR ABSORPTION COEFFICIENT

The cross sections are from Spears (1992) and are referenced to v=2.200 Km/s neutrons, with λ=1.79895 Å. Cross sections are in barns. The remainder of the quantities listed below have units as specified.

$$\mu_i = \frac{\rho(0.6022)}{MW_i} m_f \frac{\rho}{\rho_0}(\sigma_{inc} + \sigma_{abs}) \quad (3),$$

where MW_i is the molecular weight of the particular atomic species,
and m_f is the mass fraction of species i.

We assume that σ_{abs} behaves as a 1/v absorber and calculate the neutron velocity from

$$\lambda = \frac{h}{mv};\ v(Km/s) = \frac{3.95603}{\lambda(Å)} \quad (4).$$

The absorption correction can be calculated from μ, in various ways. One particularly convenient way is to use the relations in the GSAS manual (Larson and Von Dreele, 2000). This formalism has been implemented in the PDF-4+ 2014.

TABULATION OF NEUTRON INSTRUMENT RESOLUTION FUNCTIONS FOR PDF-4+

To calculate the neutron powder diffraction patterns on-the-fly, we must turn out attention to the resolution function. In the PDF-4+, there is a need to specify the resolution for all neutron pattern PDF-4+ entries. The first is the PDF card, which gives the standard reduced pattern d,I pairs for all reflections. In this case, what is required is the average weighted resolution function that can be used for the static PDF card information. This is calculated in the ICDD POWD12++ editorial program (Clark et.al, 1973, further developed at ICDD). The resolution is specified by U, V, W and the definitions needed to use this triplet are available in the GSAS manual (Larson and Von Dreele, 2000). This derives from the well-known Caglioti function:

$$\mathrm{FWHM} = \sqrt{\mathrm{variance}} = \sqrt{\sigma^2}$$

$$\text{where } \sigma^2 = \mathrm{U}\tan^2\Theta + \mathrm{V}\tan\Theta + \mathrm{W}.$$

Note that PDF-4+ entries deal with angles in degrees; whereas GSAS deals with angles in centidegrees. Table 1 shows both of these resolution functions for data published for four neutron scattering instruments.

Table 1. Instrumental resolution function quantities for four instruments specified with GSAS and with PDF-4+ DDView +.

MACHINE	WAVELENGTH	U	V	W
D1A	1.909 Å	354.11	-760.32	651.60
	PDF-4+ Pref.	0.1964	-0.4217	.3614
BT1	1.53966 Å	236.37	-283.25	167.50
	PDF-4+ Pref.	0.1311	-0.1571	0.0929
HB2A(113)	2.4111 Å	398.46	-343.2	162.99
	PDF-4+ Pref.	0.2210	-0.1903	0.0904
HB2A(115)	1.5378 Å	376.83	-510.25	273.15
	PDF-4+ Pref.	0.2029	-0.2830	0.1515
"average" U,V,W		338.70	-474.23	313.72
	PDF-4+ Pref.	0.18785	-0.2630	0.1740
"weighted" U,V,W		177.42	-240.24	162.82
	PDF-4+ Pref.	0.09840	-0.13324	0.09030

For comparison, the subsequent resolution functions are shown in Figure 1.

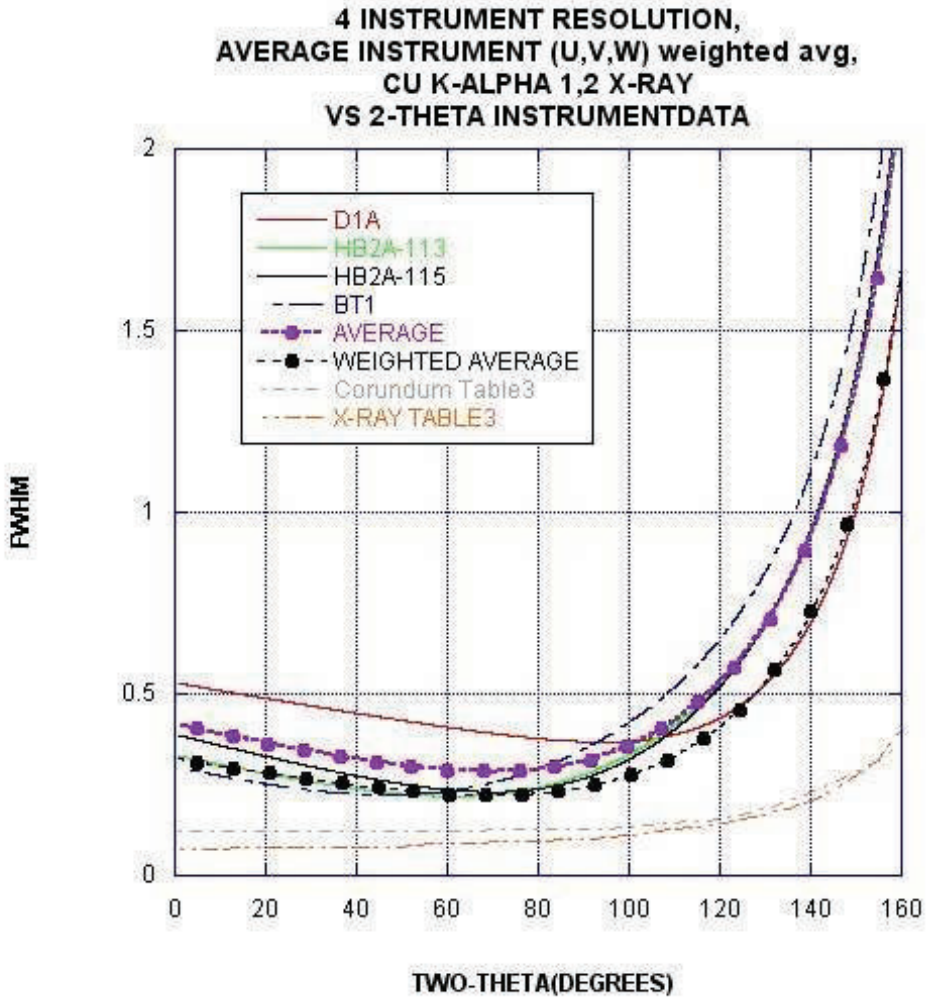

Figure 1. FWHM values as a function of two-theta (degrees). For comparison, the resolution for several in-house X-ray instruments, using corundum Al_2O_3 powder are also shown.

The instrument resolution function for d,I pairs in the PDF-4+ 2014 is based on the weighted average function in Table 1. However, for neutron diffraction (and X-rays as well) on-the-fly calculated patterns, the resolution is set by preference selection in the PDF-4+ 2014. These parameters can be adjusted to match experimental data to on-the-fly calculated patterns in the PDF-4+ 2014.

Figure 2 shows the search results for 241,000 patterns that have atomic coordinates in the PDF-4+ 2014. The d,I list for PDF number 04-006-8178, V_2O_3, result from our efforts to calculate neutron scattering patterns for all of these entries. To populate this search list requires only that

these entries have atomic structure information. On the PDF Card display, I/I_c for both X-rays and neutrons are listed.

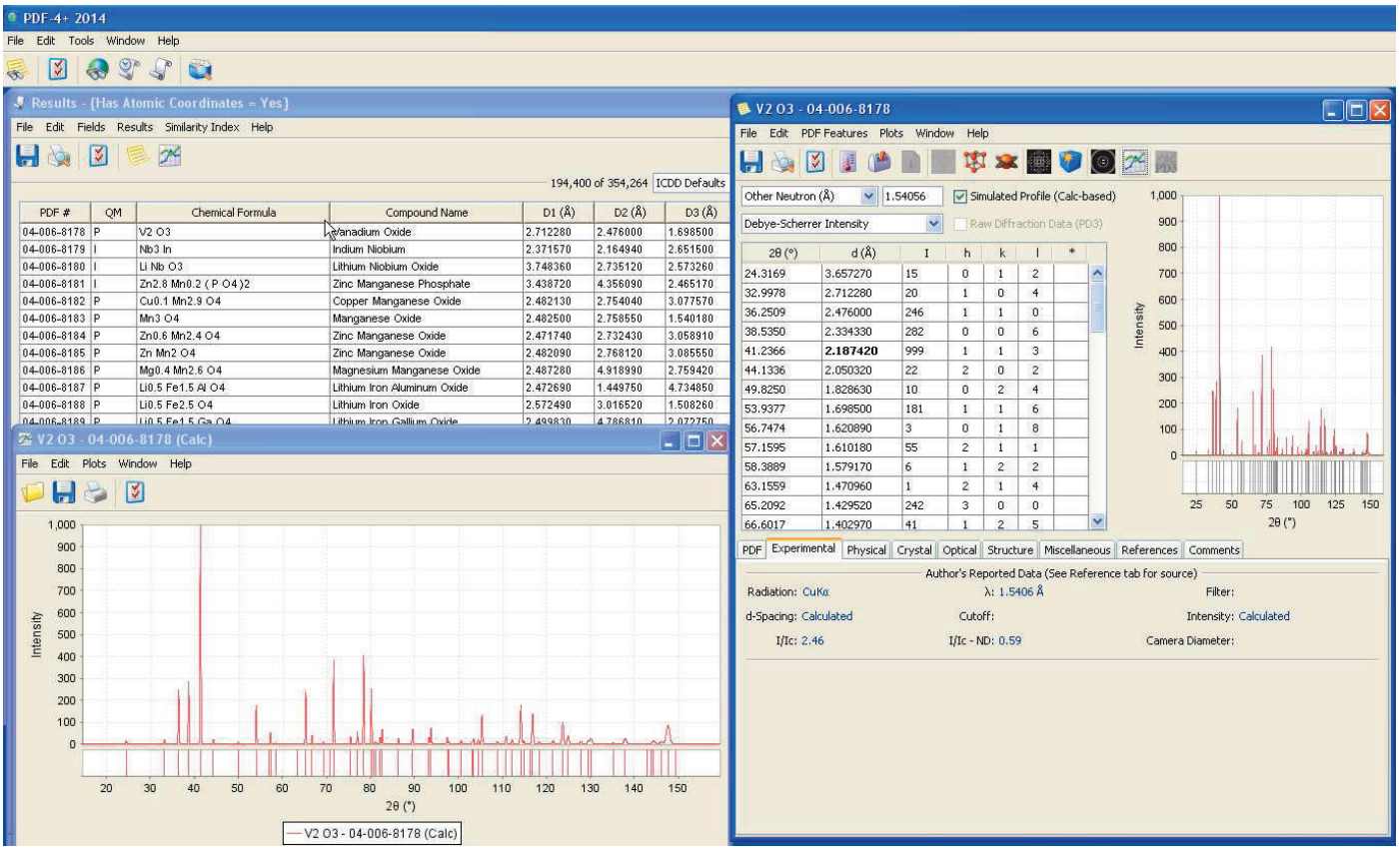

Figure 2. Search display for the PDF-4+ 2014. The search criteria select only PDF entries that have atomic coordinates. Both the PDF Card and the only-the-fly calculated pattern are for neutron diffraction patterns. The cylindrical sample has a 8mm diameter and the packing fraction is 0.6. These parameters set the absorption for the sample.

This PDF entry was chosen since for V_2O_3, the vanadium scattering length b_V=-0.03824x10^{-8}cm whereas the oxygen scattering length, b_O=0.5803x10^{-8}cm. This result is essentially a oxygen heavy atom with miniscule scattering from the vanadium atoms. In contrast, with Z_V=28 and Z_O=8, the x-ray scattering is dominated by the contributions from the vanadium atoms.

NEUTRON DATA SEARCH-INDEXING WITH THE PDF-4+ 2014

As a precursor to search/match, the Normalized R-Index Method is an extraordinarily powerful tool that can be used to discover matches between experimental data and calculated patterns in the PDF-4+. The idea is to compare an experimental neutron powder pattern with on-the-fly calculated patterns from the PDF-4+ 2014. The method is based on the following algorithm:

$$R(\text{index}) = \sum_{i=1}^{n} \left| \frac{I_i^{\text{count}}}{\sum_{j=1}^{n} I_j^{\text{count}}} - \frac{I_i^{\text{calc}}}{\sum_{j=1}^{n} I_j^{\text{calc}}} \right| \qquad (5),$$

where n refers to the number of data points, I_i^{calc} are the individual digitized values from the reference pattern (obtained using on-the-fly techniques from the PDF-4+) and I_i^{count} are digitized values from the experimental pattern of interest. The algorithm in Eq. 5 is modified from that shown by Faber and Blanton (2008) and contains a separate normalization factor for both the experimental pattern (count) and the calculated pattern (calc). The calculated patterns from the PDF-4+ are scaled to either 100 or 1000 for the peak intensity in the pattern and normalization removes consideration of this scaling. Moreover, this normalization takes into account differences in temperature factors used in the calculated patterns when compared to the experimental pattern. The range of R(index) values is: $0 \leq$ R(index) ≤ 2. The lower the index value, the better the match. Applications of the Similarity Index in the PDF-4+ can be applied to both the Search Results (DDView+) and Search-Indexing (SIeve+) search results.

The neutron diffraction data for yttrium iron garnet are available in the GSAS suite. We shall examine this data using the Normalized R-index in the PDF-4+ 2014. The data are from A. Hewat using D1A at the Institute Laue Langevin (ILL). The wavelength is 1.909 Å. The instrument resolution function is shown in Table 1. As a convenience, the search results use a priori chemical constraints that the compound chemical formula should contain Y, Fe and Al. The results of the search are illustrated in Figure 3.

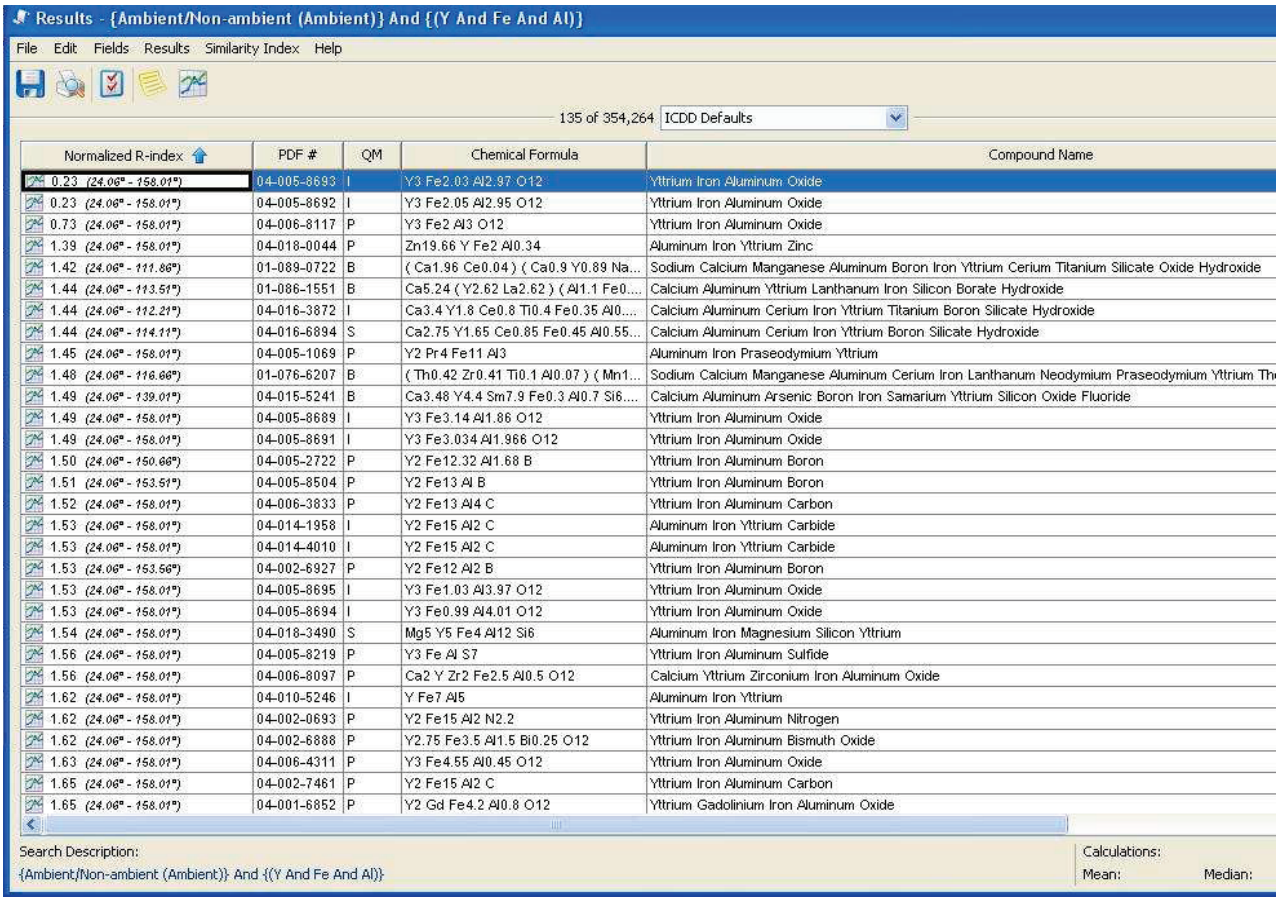

Normalized R-index	PDF #	QM	Chemical Formula	Compound Name
0.23 (24.06° - 158.01°)	04-005-8693	I	Y3 Fe2.03 Al2.97 O12	Yttrium Iron Aluminum Oxide
0.23 (24.06° - 158.01°)	04-005-8692	I	Y3 Fe2.05 Al2.95 O12	Yttrium Iron Aluminum Oxide
0.73 (24.06° - 158.01°)	04-006-8117	P	Y3 Fe2 Al3 O12	Yttrium Iron Aluminum Oxide
1.39 (24.06° - 158.01°)	04-018-0044	P	Zn19.66 Y Fe2 Al0.34	Aluminum Iron Yttrium Zinc
1.42 (24.06° - 111.86°)	01-089-0722	B	(Ca1.96 Ce0.04) (Ca0.9 Y0.89 Na...	Sodium Calcium Manganese Aluminum Boron Iron Yttrium Cerium Titanium Silicate Oxide Hydroxide
1.44 (24.06° - 113.51°)	01-086-1551	B	Ca5.24 (Y2.62 La2.62) (Al1.1 Fe0....	Calcium Aluminum Yttrium Lanthanum Iron Silicon Borate Hydroxide
1.44 (24.06° - 112.21°)	04-016-3872	I	Ca3.4 Y1.8 Ce0.8 Ti0.4 Fe0.35 Al0....	Calcium Aluminum Cerium Iron Yttrium Titanium Boron Silicate Hydroxide
1.44 (24.06° - 114.11°)	04-016-6894	S	Ca2.75 Y1.65 Ce0.85 Fe0.45 Al0.55...	Calcium Aluminum Cerium Iron Yttrium Boron Silicate Hydroxide
1.45 (24.06° - 158.01°)	04-005-1069	P	Y2 Pr4 Fe11 Al3	Aluminum Iron Praseodymium Yttrium
1.48 (24.06° - 116.66°)	01-076-6207	B	(Th0.42 Zr0.41 Ti0.1 Al0.07) (Mn1...	Sodium Calcium Manganese Aluminum Cerium Iron Lanthanum Neodymium Praseodymium Yttrium Th
1.49 (24.06° - 139.01°)	04-015-5241	B	Ca3.48 Y4.4 Sm7.9 Fe0.3 Al0.7 Si6....	Calcium Aluminum Arsenic Boron Iron Samarium Yttrium Silicon Oxide Fluoride
1.49 (24.06° - 158.01°)	04-005-8689	I	Y3 Fe3.14 Al1.86 O12	Yttrium Iron Aluminum Oxide
1.49 (24.06° - 158.01°)	04-005-8691	I	Y3 Fe3.034 Al1.966 O12	Yttrium Iron Aluminum Oxide
1.50 (24.06° - 150.66°)	04-005-2722	P	Y2 Fe12.32 Al1.68 B	Yttrium Iron Aluminum Boron
1.51 (24.06° - 153.51°)	04-005-8504	P	Y2 Fe13 Al B	Yttrium Iron Aluminum Boron
1.52 (24.06° - 158.01°)	04-006-3833	P	Y2 Fe13 Al4 C	Yttrium Iron Aluminum Carbon
1.53 (24.06° - 158.01°)	04-014-1958	I	Y2 Fe15 Al2 C	Aluminum Iron Yttrium Carbide
1.53 (24.06° - 158.01°)	04-014-4010	I	Y2 Fe15 Al2 C	Aluminum Iron Yttrium Carbide
1.53 (24.06° - 153.56°)	04-002-6927	P	Y2 Fe12 Al2 B	Yttrium Iron Aluminum Boron
1.53 (24.06° - 158.01°)	04-005-8695	I	Y3 Fe1.03 Al3.97 O12	Yttrium Iron Aluminum Oxide
1.53 (24.06° - 158.01°)	04-005-8694	I	Y3 Fe0.99 Al4.01 O12	Yttrium Iron Aluminum Oxide
1.54 (24.06° - 158.01°)	04-018-3490	S	Mg5 Y5 Fe4 Al12 Si6	Aluminum Iron Magnesium Silicon Yttrium
1.56 (24.06° - 158.01°)	04-005-8219	P	Y3 Fe Al S7	Yttrium Iron Aluminum Sulfide
1.56 (24.06° - 158.01°)	04-006-8097	P	Ca2 Y Zr2 Fe2.5 Al0.5 O12	Calcium Yttrium Zirconium Iron Aluminum Oxide
1.62 (24.06° - 158.01°)	04-010-5246	I	Y Fe7 Al5	Aluminum Iron Yttrium
1.62 (24.06° - 158.01°)	04-002-0693	P	Y2 Fe15 Al2 N2.2	Yttrium Iron Aluminum Nitrogen
1.62 (24.06° - 158.01°)	04-002-6888	P	Y2.75 Fe3.5 Al1.5 Bi0.25 O12	Yttrium Iron Aluminum Bismuth Oxide
1.63 (24.06° - 158.01°)	04-006-4311	P	Y3 Fe4.55 Al0.45 O12	Yttrium Iron Aluminum Oxide
1.65 (24.06° - 158.01°)	04-002-7461	P	Y2 Fe15 Al2 C	Yttrium Iron Aluminum Carbon
1.65 (24.06° - 158.01°)	04-001-6852	P	Y2 Gd Fe4.2 Al0.8 O12	Yttrium Gadolinium Iron Aluminum Oxide

Figure 3. Normalized R-Index search of fully digitized on-the-fly neutron diffraction patterns in the PDF-4+ 2014. The Index is defined in the help documentation for the PDF-4 and consists of full pattern comparisons between an experimental pattern and those calculated from the database.

There are 135 hits from 354,264 entries in the PDF-4+ 2014 database. The Normalized R- Index is listed in the first column of the figure; the Index would be 0.0 for a perfect fit. Note that the two lowest values of the R Index values are 0.23 and are well-separated from the other entries; the search results are unambiguous. The best total pattern match occurs for the PDF Card, 04-005-8693; the structural data are also listed (Fischer et. al 1975). The experimental and calculated best match patterns are compared in Figure 4.

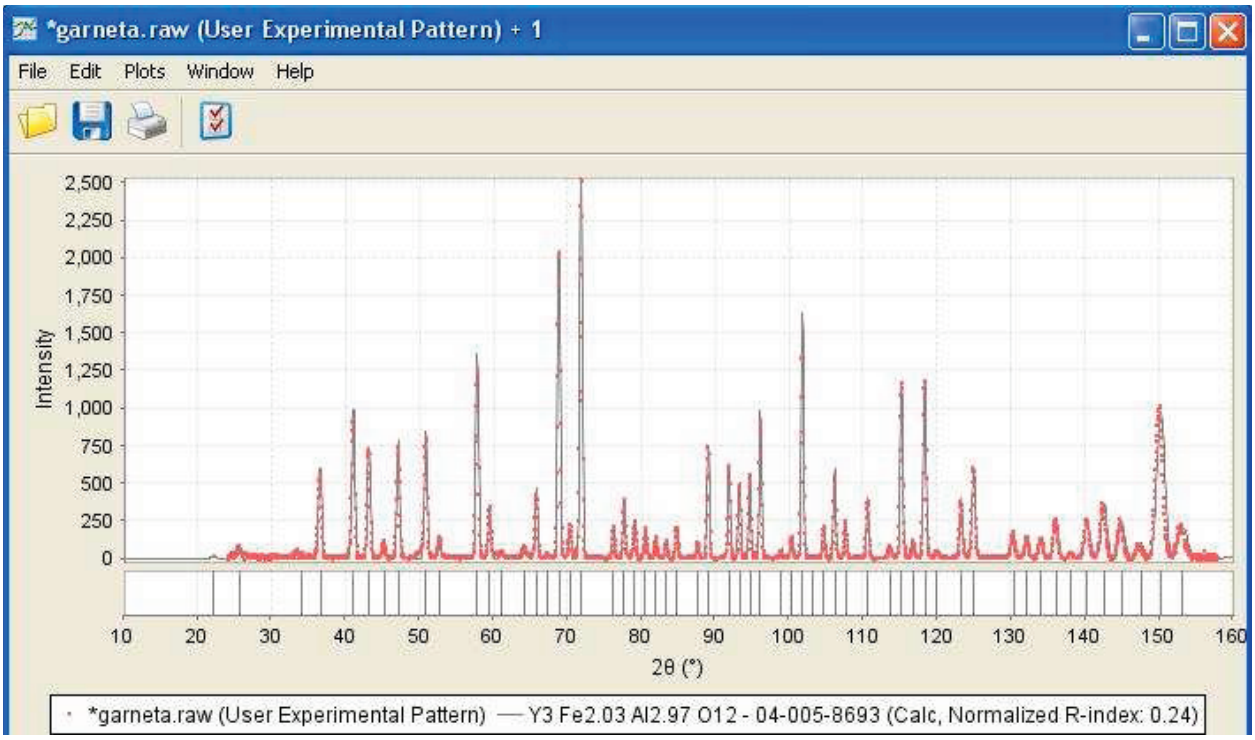

Figure 4. Comparison between experiment and calculated patterns for garnet data from D1A (Institut Laue Langevin, ILL). The Normalized R-Index=0.23 (nearly a perfect fit) for this specific entry.

There is one peak at 2-theta=22.2 degrees that is not accounted for with this model. The experimental intensity for the (211) reflection is apparently very small.

SEARCH/MATCH USING SIeve+

Using search/match methods from SIeve+ in the PDF-4+ 2014, we have analyzed neutron data kindly supplied by R. Popoular at the LLB in Saclay, France. In the PDF-4+ 2014, neutron d,I pairs are added to the database for use with Hanawalt, Fink and Long8 searches. This required calculation of ~241,000 patterns from which d,I pairs have been extracted. The search/match results are illustrated in Figure 5. It is interesting to note that applying the Normalized R-Index method described above, we obtain 0.74 for the index and this value is the lowest (best fit to the experimental data) for all patterns searched. This R-Index value corresponds to the data for PDF Card 04-017-1626, hydroxy-apatite. Using SIeve+, the search/match methods in the PDF-4+ 2014 show a detected second phase of CaO, PDF Card 04-017-9575. An estimate of the second phase abundance is 2 wt.%.

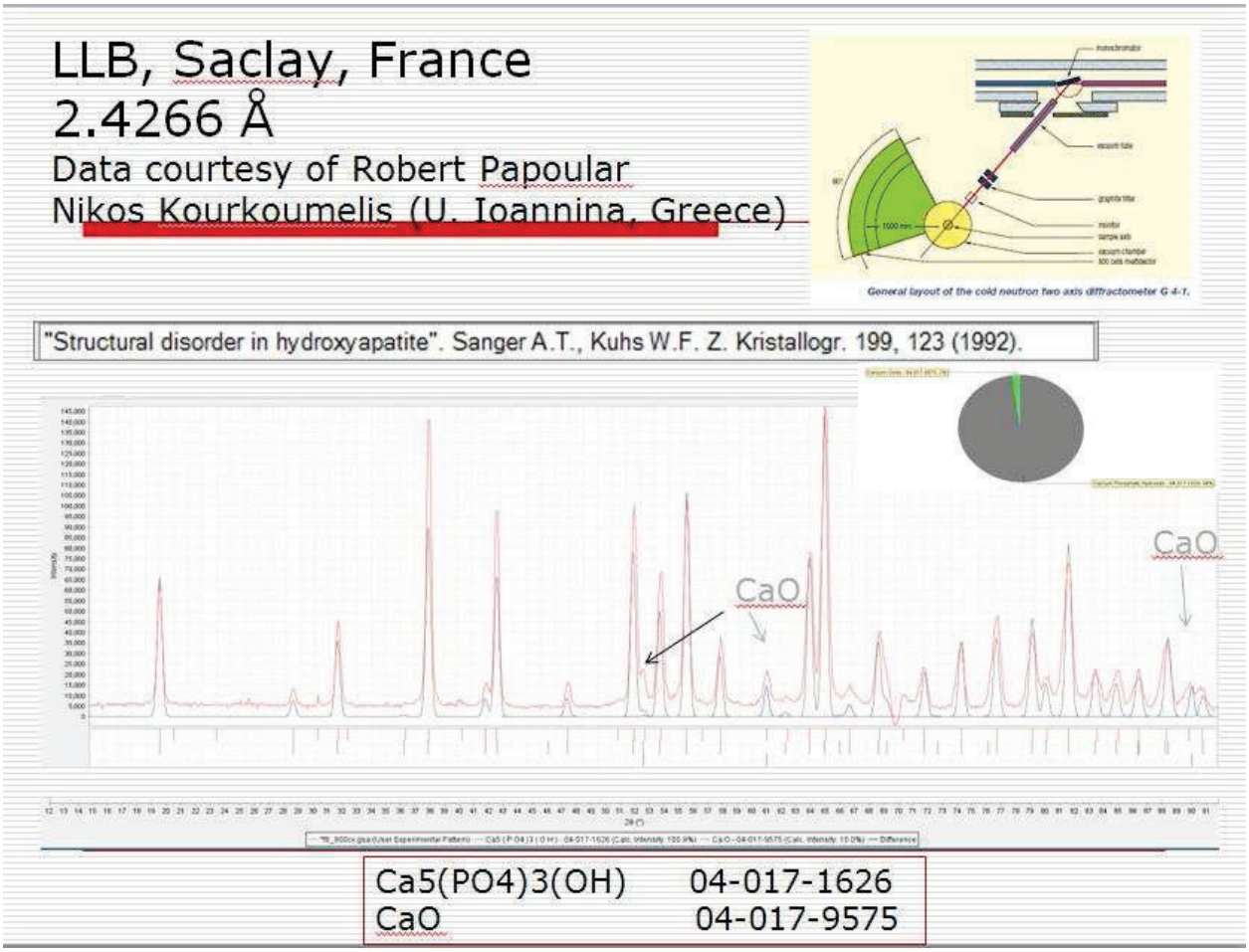

Figure 5.Multiphase analysis of from the D4-1 diffractometer on the cold source at LLB.

An additional example of search/match methods from SIeve+ in the PDF-4+ 2014, we have analyzed neutron diffraction data kindly supplied by A. Payzant from the HB-2A diffractometer at HFIR, Oak Ridge National Laboratory. The result of a 3-phase analysis is illustrated in Figure 6.

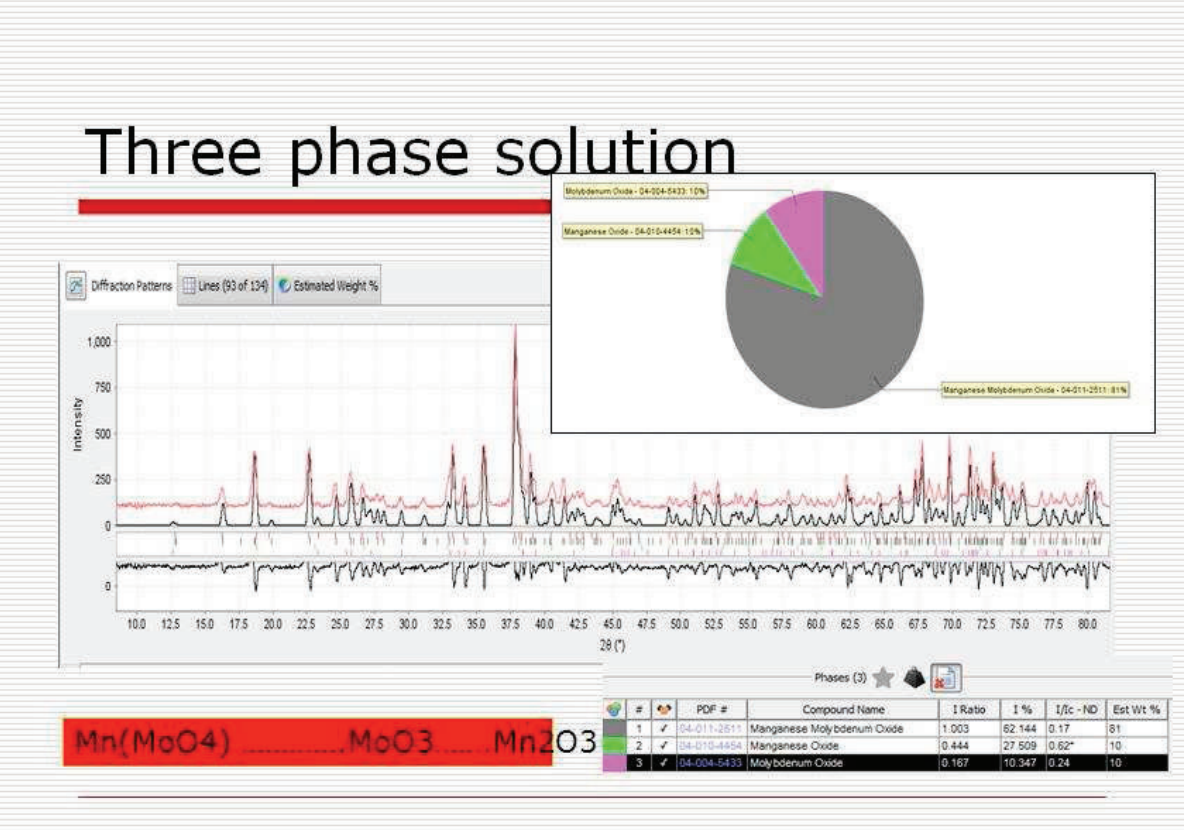

Figure 6. Three-phase analysis of neutron diffraction data taken on the HB-2A powder diffractometer at the High Flux Isotope Reactor (HFIR) at Oak Ridge National Laboratory (ORNL). Data is courtesy of A. Payzant.

The lowest Normalized R-Index for this data is 1.07 and corresponds to Mn(MoO4), PDF Card 04-011-2511. From Search/Match, the approximate abundances are MnMOO4 at 81 wt.%, Mn2O3 at 10 wt.% and MoO3 at 9 wt.%. The elevated R-Index probably arises because of the presence of 20 wt.% additional phases.

DISCUSSON

We have implemented calculation of neutron diffraction data which required that we calculate neutron powder diffraction intensities for cylindrical sample geometry, taking into account absorption effects that are energy dependent, packing density for the sample container, and the sample container diameter. In general the neutron incident beam wavelength could be selected from a significant range of neutron energies that span the Maxwellian component of the incident spectrum. We make the assumption that the scattering cross sections show a 1/v dependence and thus we ignore resonance effects.

Using copper K-alpha, λ=1.5406 Å, as the reference state, neutron values of I/I_c have been calculated for all 241,000 entries with atomic coordinates. This quantity has been calculated for laboratory source X-ray, neutron and synchrotron sources.

The PDF Card neutron derived d,I pairs are calculated with λ=1.5406 Å. To account for a broad range of instrument resolution functions available at steady-state neutron sources, we have developed a weighted average resolution function as illustrated in Figure 1. DDView+ in the PDF-4+ 2014 also provides for calculation of on-the-fly neutron powder patterns. The DDView+ preferences can be set for any instrument resolution function and this provides us with a means of comparing experimental data with calculated full patterns. There are 241,000 entries in the PDF-4 that contain structural data so that these patterns can be calculated. GSAS, FULLPROF and JANA have been used to check that the Rietveld refinements yield the starting structural parameters found in the PDF-4+ 2014.

In general, the neutron resolution function is not as sharp as for X-rays, however, we need to recognize that when compared to Cu K-alpha from laboratory sources, neutrons sources only develop singlet hkl's (compared with alpha-1,2 doublets).

For search/match, we have developed 10 d,I pairs for each pattern using Hanawalt, Fink and Long8 searches. Moreover, we have additional search/match capability using the Normalized R-Index full pattern analyses. This method works well on major phases, but needs to be developed further for weak phases. It is perhaps interesting to note that this Index total pattern method is quite successful without specific information about the sample composition. Alternatively, because the pattern comparisons are computationally intensive, Boolean filters can be used to help minimize the time to complete the analyses.

REFERENCES

Bacon, G. E. **(1975)**. Neutron Diffraction, 3rd edition (Clarendon Press Oxford), p. 112 and p. 147.

Clark. C., Smith, D. K., and Johnson, G. G. (**1973**). " A Fortran Program for Calculating X-ray Powder Diffraction Patterns, Version 5, Department of Geological sciences, Pennsylvania State University, University Park, PA. POWD12++ is Version 12 and has been subsequently developed at the ICDD.

Faber, J, Fawcett, T, (**2002)**. "The Powder Diffraction File: Present and Future," Acta Cryst. **B58**, 325-332.

Faber, J**. (2004)**. "ICDD's New PDF-4 Organic Database: Search Indexes, Full Pattern Analysis and Data Mining," Crystallography Reviews **10**, 97-107.

Faber, J. and Blanton J. **(2008)**. "Full Pattern Comparison of Experimental and Calculated Powder Patterns using the Integral Index Method in PDF-4+," Powder Diffraction **23**, 141-145. See also Hofmann, D and Kuleshova, L**. (2005)**. "New Similarity Index for Crystal Structure Determination from X-Ray Powder Diagrams", J. Appl. Cryst. **38**, 861-866.

Fischer P., Halg W., Roggwiller P., Czerlinsky E.R. (**1975)**. "Distributions of Cations in Y-Fe-Al Garnets," Solid State Commun. **16**, 987.

Hubbard, C. R., Evans, E. H., and Smith, D. K. **(1976)**. "The Reference Intensity Ratio, I/I_c for Computer Simulated Powder Patterns," J. Appl. Cryst. **9**, 169-174. The literature citations in this reference are particularly extensive.

Larson, A. C and Von Dreele, R. B. (**2000**). "General Structure Analysis System (GSAS)," Los Alamos National Laboratory Report LAUR 86-748. See also: Toby, B. H. (2001), "EXPGUI, a graphical user interface for GSAS", J. Appl. Cryst. **34**, 210-213. Note that Toby has published a number of useful web-based applications that allow calculation of absorption corrections.

Spears, V. F. **(1992)**. "Neutron Scattering Lengths and Cross Sections," Neutron News **3**, 29-37.